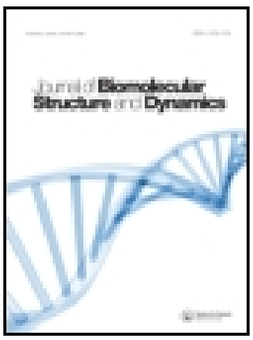

Taylor & Francis
Taylor & Francis Group

Journal of Biomolecular Structure and Dynamics

ISSN: 0739-1102 (Print) 1538-0254 (Online) Journal homepage: https://www.tandfonline.com/loi/tbsd20

Agonism activities of lyso-phosphatidylcholines (LPC) Ligands binding to peroxisome proliferator-activated receptor gamma (PPARγ)

Jiayue Wang, Bohong Wang & Yan Zhang

To cite this article: Jiayue Wang, Bohong Wang & Yan Zhang (2019): Agonism activities of lyso-phosphatidylcholines (LPC) Ligands binding to peroxisome proliferator-activated receptor gamma (PPARγ), Journal of Biomolecular Structure and Dynamics, DOI: 10.1080/07391102.2019.1577175

To link to this article: https://doi.org/10.1080/07391102.2019.1577175

Published online: 26 Apr 2019.

JOURNAL OF BIOMOLECULAR STRUCTURE AND DYNAMICS
https://doi.org/10.1080/07391102.2019.1577175

Agonism activities of lyso-phosphatidylcholines (LPC) Ligands binding to peroxisome proliferator-activated receptor gamma (PPARγ)

Jiayue Wang[a,b], Bohong Wang[b,c] and Yan Zhang[a,d]

[a]State Key Laboratory of Molecular Reaction Dynamics, Dalian Institute of Chemical Physics (DICP) Chinese Academy of Sciences, Dalian, China; [b]University of Chinese Academy of Sciences, Beijing, China; [c]CAS Key Laboratory of Separation Science for Analytical Chemistry, Dalian Institute of Chemical Physics (DICP) Chinese Academy of Sciences, Dalian, China; [d]Institute of Molecular Sciences and Engineering, Shandong University, Qingdao, China

Communicated by Ramaswamy H. Sarma

ABSTRACT

PPARγ is an isoform of peroxisome proliferator-activated receptor (PPAR) belonging to a super family of nuclear receptors and is a primary target of the effective drug to treat the type II diabetes. The experiments found that Lyso-phosphatidylcholines (LPC) could bind to PPARγ, but the binding modes remain unknown. We used the Molecular Docking and Molecular Dynamic (MD) simulations to study the binding of four LPC ligands (LPC16:0, LPC18:0, LPC18:1-1 and LPC18:1-2) to PPARγ. The two-step MD simulations were employed to determine the final binding modes. The 20 ns MD simulations for four final LPC-PPARγ complexes were performed to analyze their structures, the binding key residues, and agonism activities. The results reveal that three LPC ligands (LPC16:0, LPC18:0 and LPC18:1-1) bind to Arm II and III regions of the Ligand Binding Domain (LBD) pocket, whereas they do not interact with Tyr473 of Helix 12 (H12). In contrast, LPC18:1-2 can form the hydrogen bonds with Tyr473 and bind into Arm I and II regions. Comparing with the paradigm systems of the full agonist (Rosiglitazone–PPARγ) and the partial agonist (MRL24–PPARγ), our results indicate that LPC16:0, LPC18:0 and LPC18:1-1 could be the potential partial agonists and LPC18:1-2 could be a full agonist. The in-depth analysis of the residue fluctuations and structure alignment confirm the present prediction of the LPC agonism activities.

ARTICLE HISTORY
Received 5 November 2018
Accepted 26 January 2019

KEYWORDS
PPARγ; lyso-phosphatidylcholines; type II diabetes; docking; molecular dynamics; agonists

Abbreviations: *AF-2*: Active Function Region 2; *B3LYP*: the Becke-style Three-parameter Lee-Yang-Parr correlation functional; *H2'*: Helix2'; *H3*: Helix3; *H4*: Helix4; *H5*: Helix5; *H11*: Helix11; *H12*: Helix12; *LBD*: Ligand Binding Domain; LPC: Lyso-phosphatidylcholines; *M24*: MRL24; *MM-GBSA*: Molecular Mechanics/Generalized Born Surface Area; *MD*: Molecular Dynamics; *Nmode*: Normal Mode; *ns*: nanoseconds; *Ros*: Rosiglitazone; *PBC*: Periodic Boundary Conditions; *PDB*: Protein Data Bank; *PPAR*: Peroxisome proliferator-activated receptors; *ps*: picoseconds; *RMSD*: Root Mean Square Deviations; *SPPARM*: Selective PPARγ Modulators; *TZDs*: Thiazolidinediones

1. Introduction

Peroxisome proliferator-activated receptors (PPARs) form a sub-family of the nuclear receptors that regulate the effects of the lipidic ligands at the transcriptional level (Chawla, Repa, Evans, & Mangelsdorf, 2001). PPARγ is one of the three characterized isotypes of PPARs and plays an important role in the adipogenesis, lipid metabolism and glucose homeostasis. It is a ligand inducible receptor and a primary target for treating the type II diabetes (Ahmadian et al., 2013; Lehrke & Lazar, 2005). The full PPARγ is similar to other nuclear receptors and consists of an activation function 1 (AF-1) region, a DNA-binding domain with a C4-type zinc finger structure, a hinge region, and a ligand binding domain (LBD) (Takada & Makishima, 2015). The LBD pocket of PPARγ is rather large (>1200 Å^3) among the nuclear receptors and contains three sub-pockets (Arm I, II and III) within the distinct regions arranged in a Y-shaped form (Kroker & Bruning, 2015). Arm I extends towards the Helix12 (H12), which has the high structural conservation in the PPAR isoforms. When PPARγ forms the heterodimer with another ligand-activated nuclear receptor, the retinoid X receptor, the transcriptional process will be initiated for the PPARγ targeted genes. Although the PPARγ function can be regulated by the post-transcriptional modulation, the ligand binding keeps the uppermost regulation mechanism in cells. PPARγ has a wide spectrum binding ligands. The ligand binding would trigger a conformational change of LBD to form the three-dimensional activation function-2 (AF-2) surface including the Helix3 (H3), Helix11 (H11), H12, and loop between the H3 and Helix4 (H4). This induces the dissociation of the corepressor complex and the association of a coactivator complex (Ahmadian et al., 2013).

CONTACT Yan Zhang zhangyanhg@dicp.ac.cn State Key Laboratory of Molecular Reaction Dynamics, Dalian Institute of Chemical Physics (DICP) Chinese Academy of Sciences, Dalian 116023, China

Supplementary information for this article can be accessed https://doi.org/10.1080/07391102.2019.1577175.

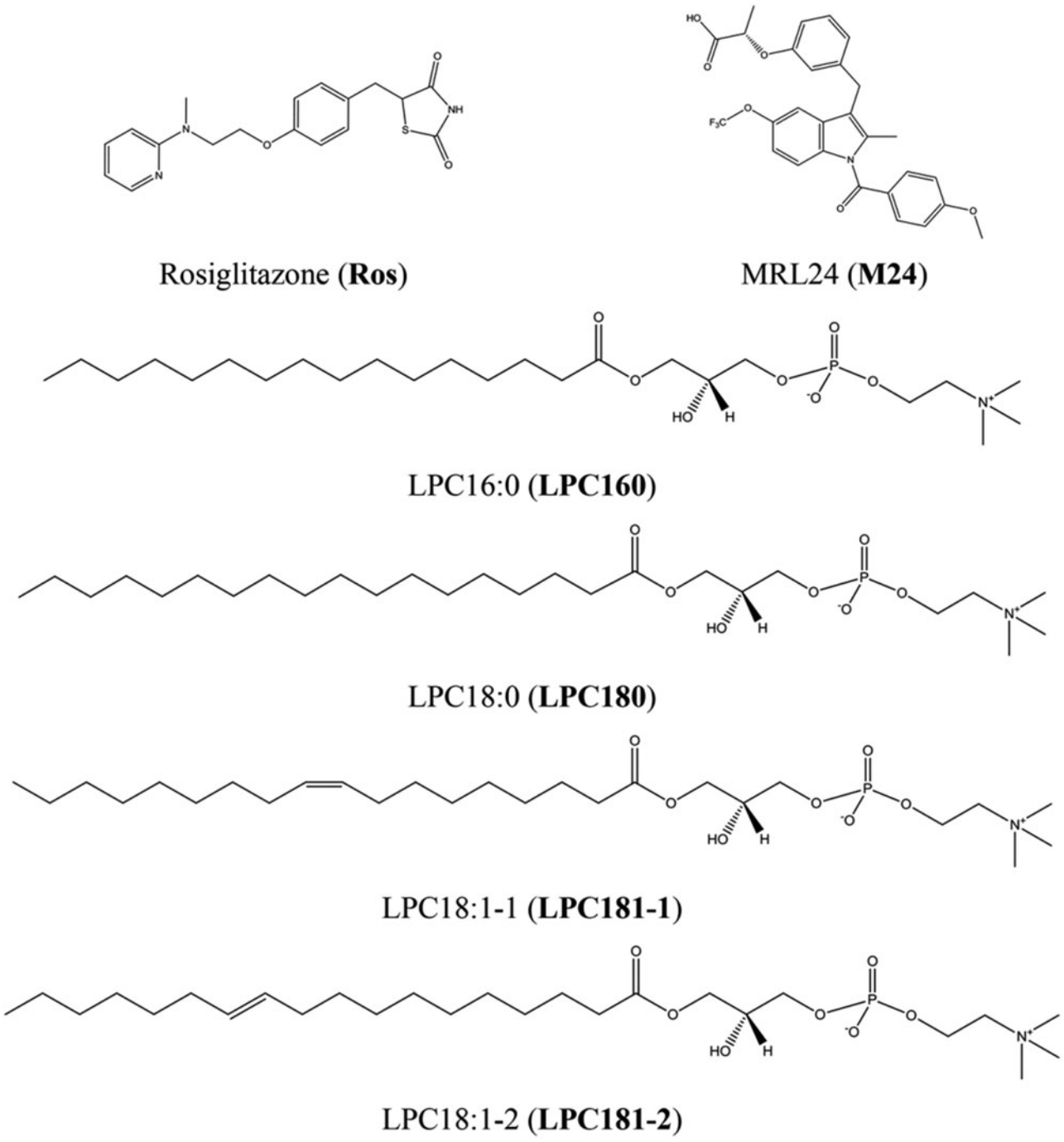

Scheme 1. Structures of six ligands including Rosiglitazone, MRL24, and four Lyso-phosphatidylcholines (LPC) ligands.

The H12 stabilization induces the AF-2 transcription activation at C-terminal region (Zoete, Grosdidier, & Michielin, 2007). The PPARγ agonists can be classified into full agonists and partial agonists. The full agonists would form the hydrogen bonding network with Arm I to directly stabilize the H12 and active AF-2 region. The activation mechanism of the partial agonist is not directly related to H12 and its binding would stabilize the regions such as the β-sheet to obtain the hypoglycemic effect (Bruning et al., 2007).

Thiazolidinediones (TZDs) are the synthetic PPARγ ligands which can effectively treat the type II diabetes and have the unique efficiency to improve the insulin sensitivity and glucose control (Day, 1999; Pearson et al., 1996). However, TZDs produce harsh side effects in pharmaceutical use. The severe side effects including weight gain, bone loss and congestive heart failure lead to the TZDs' withdrawal from the market or restricted clinical application (Ahmadian et al., 2013; Nissen & Wolski, 2007). Thus, the discovery of the novel ligands is urgent (Li et al., 2008). The natural products are the promising source of the structure pool in the advance drug design. At present, the most identified natural PPARγ ligands are the food source and have weak binding effects. Their metabolites could be the better PPARγ ligands due to the higher binding affinity (Mueller & Jungbauer, 2008; Wang et al., 2014). Natural ligands such as honokiol, amorfrutin 1, amorfrutin B and amorphastilbol have been demonstrated that

Table 1. Binding enthalpy energies of the nine models from docking simulation in the selections of two steps (in kcal/mol).

	LPC160		LPC180		LPC181-1		LPC181-2	
	2 ns	10 ns	2 ns	10 ns	2 ns	21 ns	2 ns	10 ns
Model 1	−45.4	n/a	−56.0	n/a	−48.7	n/a	−42.8	n/a
Model 2	−45.4	n/a	−54.3	n/a	−44.1	n/a	**−65.2**	−72.1
Model 3	−44.4	n/a	−52.0	n/a	**−58.1**	−57.5	−43.4	n/a
Model 4	**−57.0**	−59.9	**−64.4**	−53.1	−49.1	n/a	−53.4	n/a
Model 5	−49.7	n/a	**−69.3**	−64.5	**−52.8**	−67.3	**−65.3**	−65.5
Model 6	−45.3	n/a	**−62.0**	−66.9	**−58.8**	−61.5	−35.6	n/a
Model 7	−47.8	n/a	−51.7	n/a	−44.8	n/a	**−71.2**	−64.1
Model 8	−40.8	n/a	−48.2	n/a	−49.8	n/a	−51.3	n/a
Model 9	**−52.3**	−50.7	−54.7	n/a	−51.8	n/a	−55.8	n/a

they can improve the blood glucose levels and other relevant parameters in the diabetic animal models and have less adverse effects such as hepatomegaly, osteoblastogenesis and fluid retention (Atanasov et al., 2013; Lee, Ham, Kwon, Kim, & Kim, 2013; Weidner et al., 2012; Weidner et al., 2013). Amorfrutin 1 has the optimal targeting efficiency and the unique interference with PPARγ Ser273 phosphorylation in the visceral white adipose tissue of diet-induced obesity mice (Weidner et al., 2012). Natural ligands that display the partial agonistic effects on the PPARγ are especially employed to explore the potentiality as selective PPARγ modulators (SPPARMs; Wang et al., 2014). These modulators serve as promising candidates for drug design treating type II diabetes. For the natural PPARγ ligands, the largest category contains the oxidized low-density lipoprotein metabolites (Schupp & Lazar, 2010).

Lyso-phosphatidylcholines (LPC) are the hydrolysis products of phosphatidylcholines, which are the major component of the biological membranes. Their physiological roles include phagocyte recruitment and endothelial cells stimulation (Lauber et al., 2003; Li et al., 2016; Li et al., 2018). The recent work reported that three LPC ligands, denoted by LPC16:0, LPC18:0 and LPC18:1, can interact with PPARγ (Qin et al., 2019). LPC16:0 (LPC160) has 16 carbon atoms in its aliphatic chain and zero unsaturated bond. LPC18:0 (LPC180) and LPC18:1 both has 18 carbon atoms in their aliphatic chains. The numbers of their unsaturated bonds respectively are zero and one. LPC18:1 has two isotypes (LPC181-1 and LPC181-2) of which the double bond locates in the different position. The structures of the ligand molecules are shown in Scheme 1. It has been proved that their binding can induce the conformational change of PPARγ-LBD. Because the crystalized structure of the ligand–protein complex and NMR dynamics illustration are absent, the mechanism of the interaction between these LPC ligands and PPARγ is ambiguous. Thus we explored the binding modes between the LPC ligands and PPARγ-LBD using the molecular modeling and dynamic simulations which are the powerful and efficient tools to compute the interaction and dynamic behavior for ligand–protein complex *in silico*. They have been successfully applied in the ligand recognition, PPAR-related ligand identification and analysis of the dynamic performance and ligand–receptor interaction (Álvarez-Almazán et al., 2017; Muñoz-Gutiérrez, Sepúlveda, Caballero, Palomo, & Fuentes, 2017; Muralikumar, Vetrivel, Narayanasamy, & N. Das, 2017; Tsakovska et al., 2014; Al Sharif et al., 2017; Jia et al., 2018; Liu et al., 2018; Sharifi & Ghayeb, 2018; Singh & Mohanty, 2018). We analyzed the details of the binding behavior and identified the potency of the LPC ligands as the full agonist or partial agonist. Our simulations provide useful information to better understand the ligand-receptor interaction between the LPC ligands and PPARγ-LBD.

2. Models & computational details

In the study, we investigated binding modes of four LPC ligands (LPC160, LPC180, LPC181-1 and LPC181-2) to PPARγ-LBD. All the LPC ligands were optimized at level of the B3LYP theory (Becke, 1992, 1993; Lee, Yang, & Parr, 1988) with 6-31 + G(d) (Ditchfield, Hehre, & Pople, 1971) and 6-311G(d) basis set using the Gaussian09 package (Frisch et al., 2010). We fitted parameters of the bonds, angles, dihedrals and van der Waals of the ligands which employed in the MD simulations (Bayly, Cieplak, Cornell, & Kollman, 1993; Case et al., 2017; Wang, Wolf, Caldwell, Kollman, & Case, 2004). The X-ray crystal structure of *homo sapiens* PPARγ-LBD was obtained from the PDB file (ID: 2PRG) and chain A (residue 207-476) was retained (Nolte et al., 1998). The PDB file without the ligand is used as receptor structure for Molecular Docking. The PDB file that contains the Rosiglitazone (Ros) ligand is the reference system of the full agonists. MRL24 (M24) co-crystal system (PDB ID:2Q5P) is the reference of the partial agonists (Bruning et al., 2007). Scheme 1 displays the Ros and M24 structures. The initial conformation of Apo-system was taken from the PPARγ-LBD structure file with no ligand (PDB ID: 1PRG) (Nolte et al., 1998). Homology modeling based on the original crystal structures was performed by the online server SWISS-MODEL (Biasini et al., 2014) in order to patch up the missing segments. The protonation states of the titratable residues were determined according to the pKa values predicted by PDB2PQR online server (Dolinsky et al., 2007). We employed the Amber16 packages (Case et al., 2017) with the casual force field ff14SB (Lindorff-Larsen et al., 2010) to add the missing hydrogen atoms and optimize their positions.

After we set up the initial structures of the ligands and receptors, Molecular Docking was carried out to obtain a series of conformations using individual binding process. The Auto-Dock Vina program and the default parameters were used in the simulation (Trott & Olson, 2010). Size of the

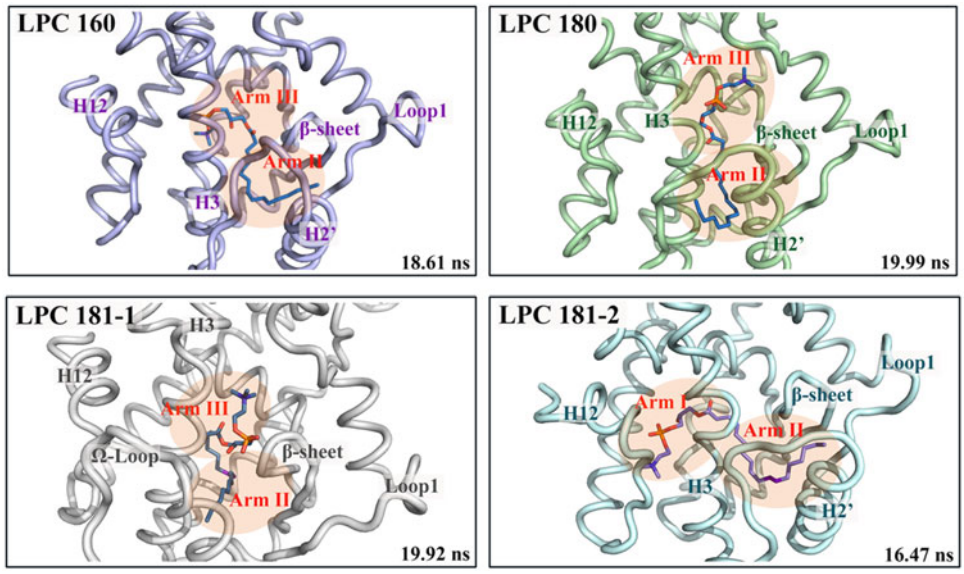

Figure 1. Structures of four LPC ligands (LPC160, LPC180, LPC181-1 and LPC181-2) binding to PPARγ.

docking box was set to embrace the complete binding pocket of PPARγ-LBD. Repeated several times, binding models of each LPC ligand towards PPARγ were assembled. The structure information of each model and a backbone RMSD value measured from comparison with the initial input conformation were recorded. When two models of the same ligand had the RMSD value difference less than 0.5, these docking models were clustered in the same group. The representative model from each group was determined by the relative binding energy. In this way, nine models were finally selected as docked conformations for each LPC ligand.

The every binding model of LPC–PPARγ complex was then fully solvated in the truncated-orthorhombic-shaped boxes. The solvation thickness is at least 12 Å. Sodium ions were added to ensure the neutrality and the water molecules were treated by the TIP3P model (Jorgensen, Chandrasekhar, Madura, Impey, & Klein, 1983). After the dissolution, we performed the minimizations to stabilize the system and release the stress. Subsequently, the MD simulation of an isocore condition was run for 200 picoseconds (ps) to heat the system to 300 K. At 300 K, the 200 ps equilibration was carried out to stretch hydrogen and side chains. Finally, the 2 nanoseconds (ns) and 20 ns MD simulations were respectively performed to determine the binding model for one LPC–PPARγ complex. In order to reduce the computational cost, the MM-GBSA binding enthalpy calculation was employed to filter the binding models (Kollman et al., 2000; Kuhn & Kollman, 2000; Miller et al., 2012). Moreover, we calculated the binding free energy of the final binding model for each LPC–PPARγ complex. Entropy contribution was estimated by the expensive normal node (Nmode) analysis (Genheden, Akke, & Ryde, 2014; Sun et al., 2018). The long-range electrostatic interactions were computed by the particle mesh Ewald method (Essmann et al., 1995). The periodic boundary conditions (PBC) and SHAKE (Ryckaert, Ciccotti, & Berendsen, 1977) algorithm were applied in the simulation. The Amber16 package was employed to perform the MD simulations (Case et al., 2017).

3. Results and discussions

For validation of the docking protocol, we performed re-docking analysis for the ligands from paradigm systems. The re-docked Ros and M24 ligands are well superimposed with the crystallized conformations. The backbone RMSD for the Ros and M24 re-docking analysis are 0.24 and 0.26, respectively. The superimposed ligand structures are shown in Supplementary Figure S1.

For each LPC–PPARγ complex, we first computed the MM-GBSA binding enthalpy energies of the nine models based on the 2 ns MD simulations. Table 1 lists the binding enthalpies of all four LPC–PPARγ systems. The lower energies were were boldfaced. Furthermore, the 20 ns MD simulations were carried out for the models with the lower binding enthalpy energies. We again calculated the binding enthalpies of the models according to the 10–20 ns MD trajectories. Observing the 10 ns binding energies in Table 1, the binding modes of three LPC ligands (LPC160, LPC181-1 and LPC181-2) could be directly determined because of the presence of the distinct lower binding energies. They are the Model 4 for LPC160, Model 5 for LPC181-1 and Model 2 for LPC181-2, respectively. For ligand LPC180, Model 5 (–64.5 kcal/mol) and Model 6 (–66.9 kcal/mol) have the close enthalpies. We further computed the binding enthalpies of the two models based on the last 5 ns MD trajectories. The binding energy of Model 6 is –66.6 kcal/mol and it is –62.8 kcal/mol for Model 5. Here we consider Model 6 as the represent binding mode of the LPC180-PPARγ complex. In the present MD simulations, the selected systems reached their equilibrium states after 4 ns according to RMSD values and the converged RMSD is ∼2 Å (Supplementary Figure S2).

Moreover, we computed the MM-GBSA binding free energies of the final binding modes including the entropy contribution (see Supplementary Table S1). The final binding free energies suggested that all the four LPC ligands can form the stable complexes with PPARγ. The result is consistent with the recent experiments (Qin et al., 2019). After the

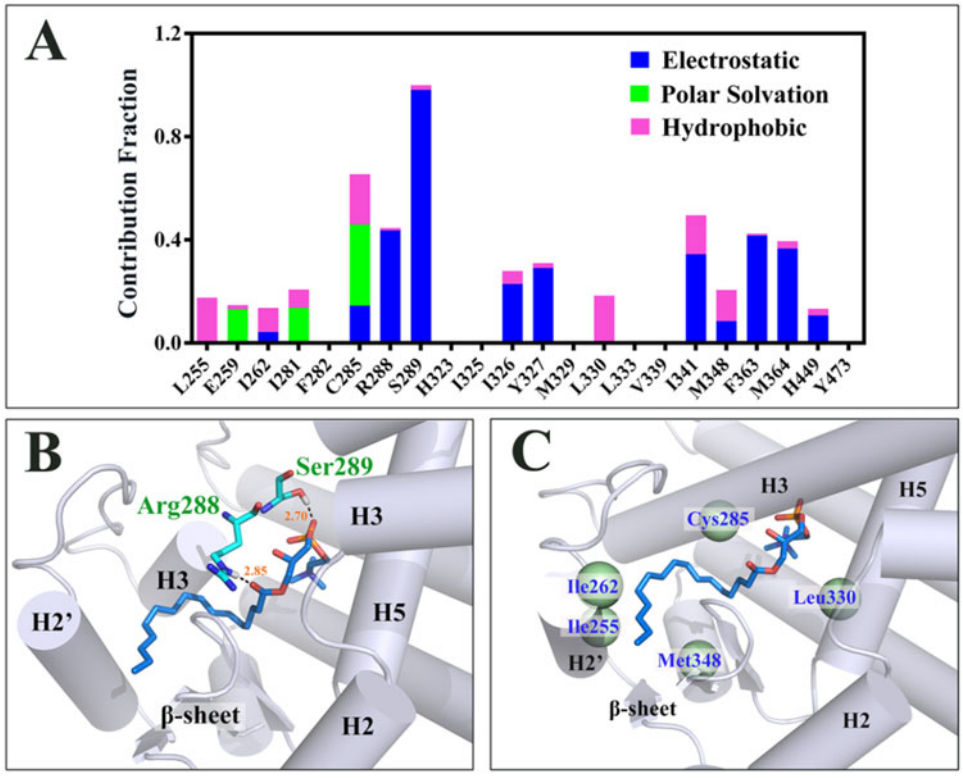

Figure 2. Energy decomposition analysis and the position of the key residues for the LPC160–PPARγ complex. Panel B presents the residues forming the interaction of the hydrogen bonds and panel C shows the residues with the hydrophobic interactions.

binding modes of the LPC–PPARγ complex were determined, we analyzed the structural properties of the LPC160–PPARγ, LPC180–PPARγ, LPC181-1–PPARγ and LPC181-2–PPARγ complexes. The LBD of PPARγ can be sterically divided into three pockets, which respectively are Arm I, Arm II and Arm III. The LPC ligand would interact with the sub-pockets to form the stable LPC–PPARγ complex. Figure 1 displays the structures of the four LPC–PPARγ complexes. The representative frames were randomly taken from the trajectories of last 5 ns in the 20 ns MD simulations.

We observe Figure 1 and can find that the LPC160 ligand resides in the regions of the Arm II and III. The binding location of another saturated LPC ligand, LPC180 resembles that of LPC160. The LPC180 ligand occupies the region of PPARγ-LBD delimited by H3 and β-sheet. LPC181-1 and LPC181-2 both have one un-saturated double bond. LPC181-1 binds into the cavity of LBD pocket in the shape of 'Ω' and locates the region of the Arm II and III. In the LBD pocket of PPARγ, LPC181-2 extends its structure in a rather linear form. The ligand crosses the H3 and is embedded into Arm I to form a close contact with the H12. The structure of the LPC181-2–PPARγ complex reveals that LPC181-2 binds to the Arm I and II. The systems including the Ros and M24 ligands are the paradigms and their binding structures are showed in Supplementary Figure S3. As shown in the figure, the regions of the M24 binding are Arm II and III. Ros binds to Arm I and II of the PPARγ-LBD pocket. Comparing Figure 1 and Supplementary Figure S3, it could be found that the structure of the LPC181-2 binding model is similar to the Ros–PPARγ complex. The M24 and other three LPC (LPC160, LPC180 and LPC181-1) ligands have the similar binding regions.

The Ω-loop (Residue 265–276), H3 (Residue 277–302), β-sheet (Residue 336–350), H12 (Residue 460–476) are the important regions within the binding site in the ligand-receptor interaction of PPARγ. The key amino acid residues would have more contribution to the binding of the ligands. In order to get the detailed understanding about the binding of four LPC ligands, we performed the energy decomposition analysis for the Ros–PPARγ, M24–PPARγ and four LPC–PPARγ complexes. Supplementary Figures S4 and S5 present the results for Ros–PPARγ and M24–PPARγ. The most remarkable difference between the two paradigm complexes is whether Tyr473 plays the dominant role in the ligand–receptor interaction. Furthermore, the contributions of the β-sheet and its connecting region (Residue 325–342) to ligand–receptor interaction are inconsistent for these two complexes.

We also analyze the polar interaction to form the hydrogen bond between the LPC ligands and PPARγ. Supplementary Table S2 lists the stable hydrogen bonds. Figure 2 shows the contributions of the residues for the LPC160–PPARγ complex and the positions of the key residues. Observing Figure 2A, we find that the most significant contribution of the ligand–receptor interaction is the electrostatic interaction produced by Ser289. During the 20 ns simulation, LPC160 forms stable hydrogen bond with Ser289 which the averaged length is 2.7 Å (Supplementary Table S2). There are also the large electrostatic interaction between Arg288 and LPC160 (Figure 2A). Arg288 and Ser289 are located in the H3 and both form the hydrogen bonds with the polar head of LPC160 (Figure 2B). The key residues,

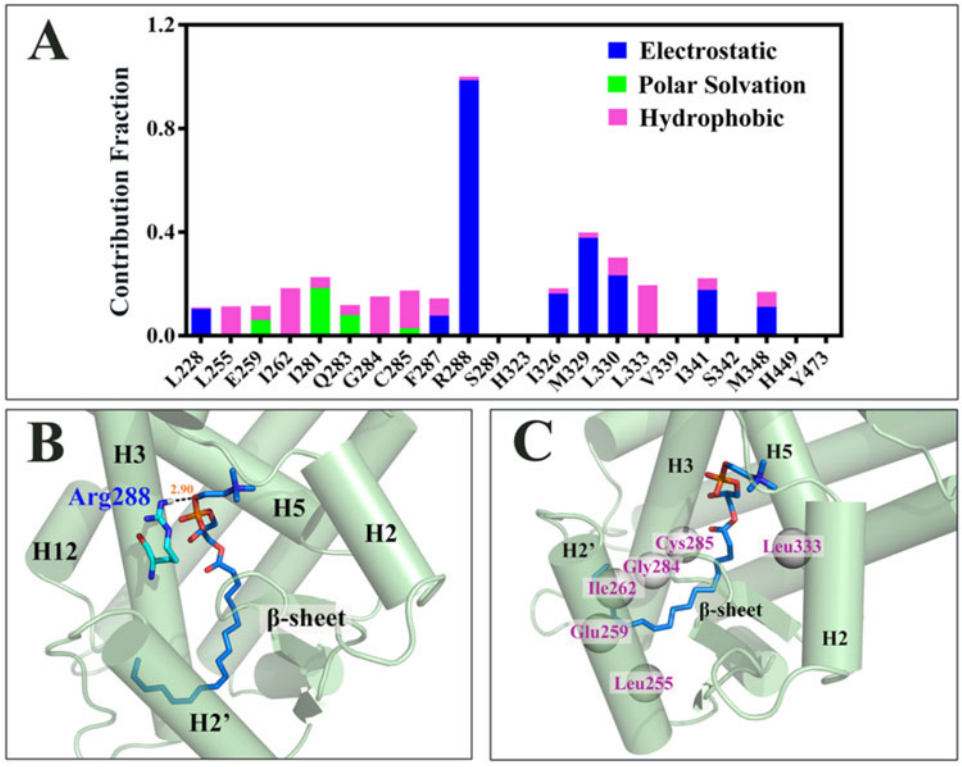

Figure 3. Energy decomposition analysis and the position of the key residues for the LPC180–PPARγ complex.

which produce the hydrophobic interaction are Ile255, Ile262, Cys285, Leu330 and Met348 (Figure 2A). They are distributed around the LPC160 to embrace the non-polar aliphatic chain of the ligand (Figure 2C). As the LPC160 ligand does not interact with the residues (His323, His449 and Tyr473) that stabilize the AF-2 region (see Supplementary Figure S4), it could predict that LPC160 may be a partial agonist.

For LPC180, we firstly selected Model 6 as the representative binding mode based on the lower binding energy it possesses. Since energy differentiation is not significant enough to distinguish Model 6 as the final binding mode of LPC180 towards PPARγ, we have analyzed the different binding modes of Model 5 and Model 6. From the alignment results of the two models (shown in Supplementary Figure S6), ligands from both models occupy mainly Arm II, and have no direct contact with H12. The only difference of the ligand binding in cavity is the orientation of the polar head. Indicated by the paradigm system, both binding modes, Model 5 and Model 6, predict LPC180 to be a partial agonist. As Model 6 is more thermodynamics favoring during the 20 ns dynamical simulation, we stick to this model as the representative binding mode of LPC180-PPARγ.

The energy decomposition analysis of LPC180–PPARγ in Figure 3 reveals that Arg288 is the most dominant residue in the ligand-receptor interaction (Figure 3A). Since Agr288 is the only residue that forms stable hydrogen bond with LPC180 in the MD simulation (Supplementary Table S2), it is clear that Arg288 has the significant contribution to the LPC180–PPARγ system. Being different from the binding mode of LPC160, LPC180 forms the hydrogen bond with Arg288 at the oxygen atoms within phosphoric acid instead of carbonyl (Figure 3B). The polar head of LPC180 is thus driven towards Helix 5 (H5). The residues that produce the hydrophobic contribution to the ligand-receptor interaction are Ile255, Glu259, Ile262, Gly284, Cys285 and Leu333 (Figure 3A). Such non-polar interactions of the residues wrap around the non-polar tail of LPC180. The ligand is strongly influenced by the hydrophobic interaction from the H2', H3 and H5 region (Figure 3C).

Figure 4 exhibits the energy decomposition and the positions of the key residues for the LPC181-1–PPARγ complex. The most distinct energy contribution is also produced by Arg288 (Figure 4A). The residue forms the strong hydrogen bond with LPC181-1 (Supplementary Table S2). LPC181-1 also interacts with Glu343 and forms the stable hydrogen bond at the oxygen atom within the phosphoric acid (Supplementary Table S2 and Figure 4B). The interaction has the considerable contribution to the ligand induce stabilization (Figure 4A). It is notable that Ile341 and Ser342 also have the remarkable electrostatic contribution. Since we don't observe the direct polar interactions between these two residues and LPC181-1 (Supplementary Table S2), their energy contribution to the system may come from the interaction with other residues. The residues of hydrophobic interaction are Cys285, Ile326, Tyr327, Leu330, Leu333, Met348 and Met364. These residues envelop the non-polar tail of the ligand (Figure 4C). No interaction between LPC181-1 and Tyr473 suggests that the LPC181-1 ligand may serve as a partial agonist.

Figure 5 displays the results of the LPC181-2–PPARγ complex. The energy decomposition result reveals that His449 and Tyr473 produce the major contribution to the LPC181-2–PPARγ stabilization (Figure 5A). They form the hydrogen

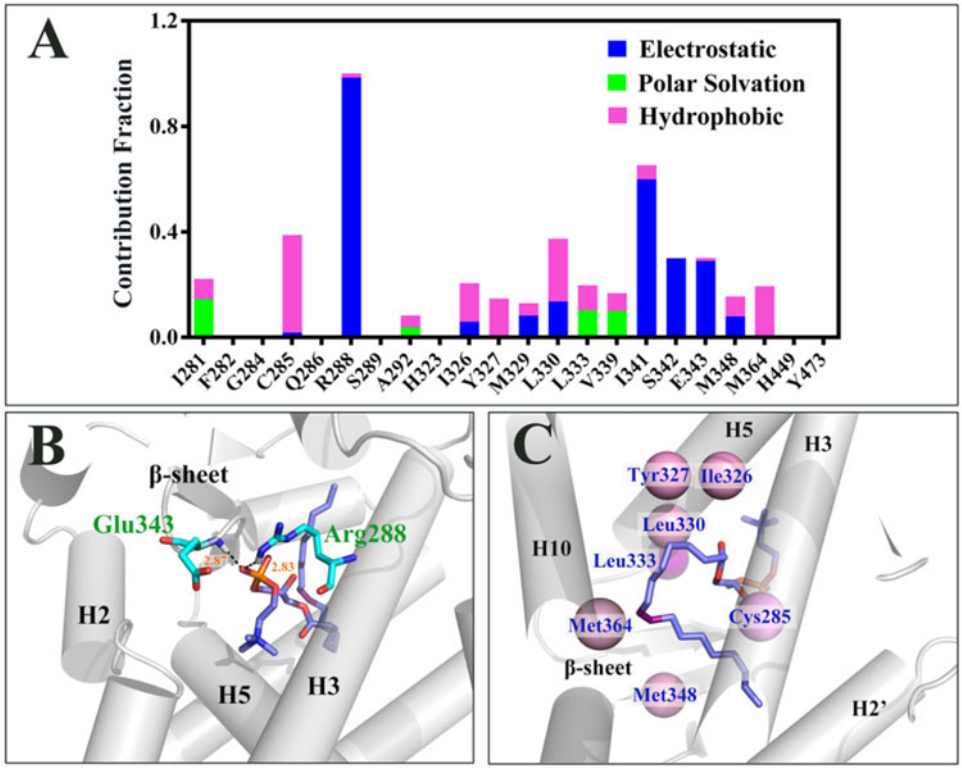

Figure 4. Energy decomposition analysis and the position of the key residues for the LPC181-1–PPARγ complex.

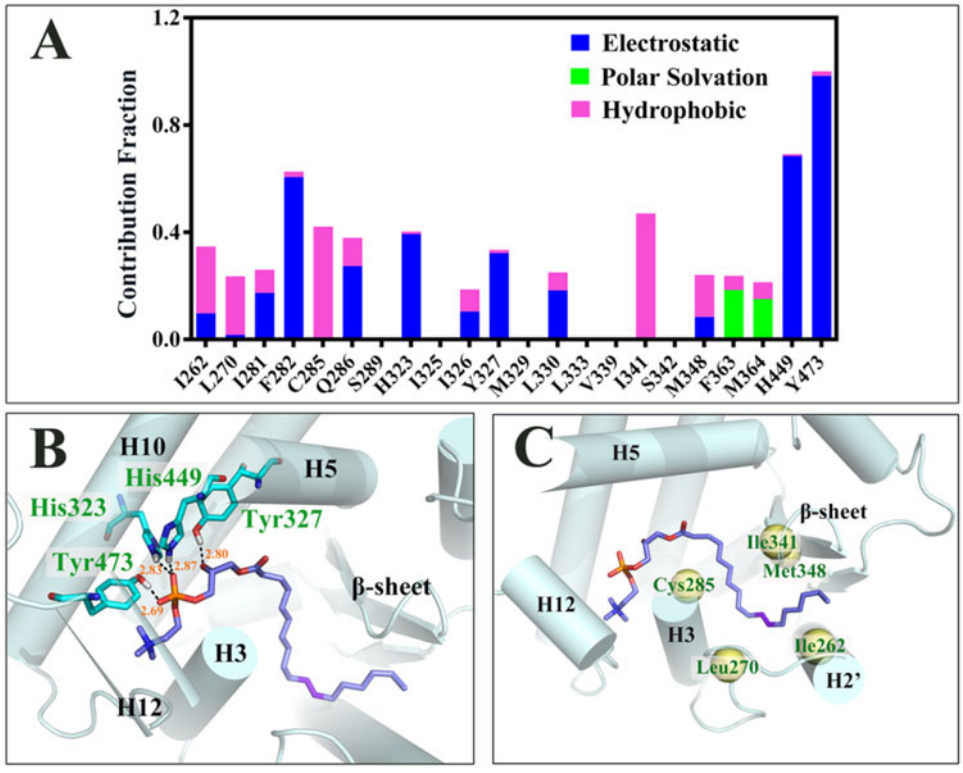

Figure 5. Energy decomposition analysis and the position of the key residues for the LPC181-2–PPARγ complex.

bonds with the polar head of LPC181-2 (Supplementary Table S2). During the 20 ns simulation run, LPC181-2 also interacts with His323 and Tyr327 by the hydrogen bonds formation (Supplementary Table S2). The two residues make notable contribution to the ligand–receptor interaction (Figure 5A). Resided in H5, H10 and H12, these residues keep the polar head of LPC181-2 penetrating in Arm I. Thus LPC181-2 has the direct interactions with H12 and AF-2

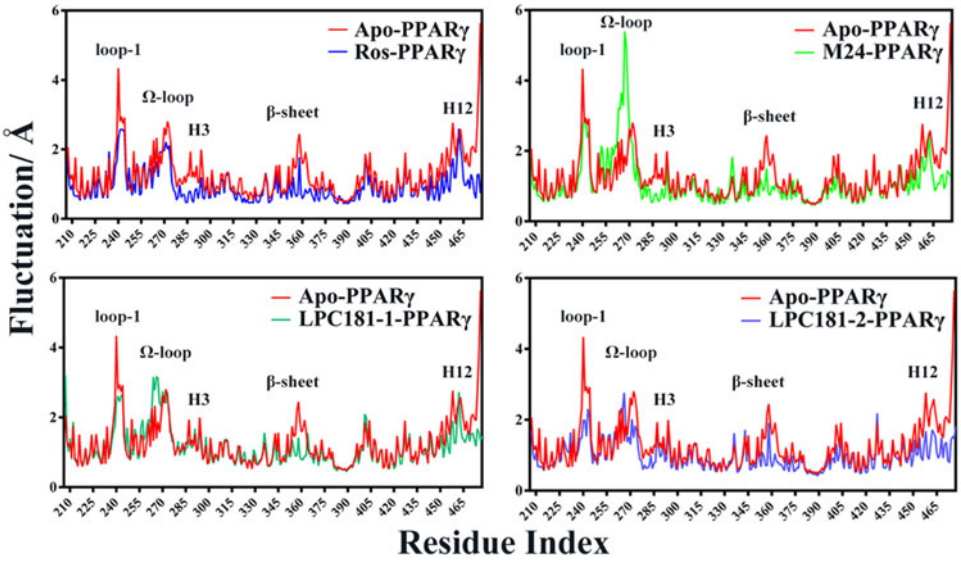

Figure 6. Residue fluctuation of the Ros–PPARγ, M24–PPARγ, LPC181-1–PPARγ and LPC181-2–PPARγ complexes during the MD simulation.

(Figure 5B). Tyr473 is the critical residue to identify the full agonists (Zoete et al., 2007). Therefore, LPC181-2 is predicted to be a full agonist. The hydrophobic interactions of LPC181-2 with PPARγ are mainly produced by Ile262, Leu270, Cys285, Ile341 and Met348, which are round the non-polar tail of the LPC ligand (see Figure 5C).

Generally, the interactions of the LPC160, LPC180 and LPC181-1 binding are similar to M24 and they could be the partial agonists. The LPC181-2 and Ros binding have the analogous features and LPC181-2 may be a full agonist. The agonism activities of four LPC ligands determined by the energy decomposition analysis (Figures 2–5) are in good agreement with the results of their binding modes (Figure 1). It has been accepted that PPARγ is an enzyme of the allosteric regulation (Zoete et al., 2007). The NMR investigations revealed that the classical full agonists could remarkably affect the H12 stabilization and induce the conformational change of the whole enzyme. In contrast, the partial agonists stabilize the regions as β-sheet and/or Ω-loop (Bruning et al., 2007; Hughes et al., 2014). Such distinct effect of the PPARγ ligands on receptor raises the possibility to identify the agonism properties of the ligands on the basis of the conformation dynamics.

The undulation of the atomic positions determines the residue fluctuation which describes the motion of the protein. We calculated the inherent residue fluctuation of the LPC181-1–PPARγ and LPC181-2–PPARγ complexes during the MD simulation to illustrate the instabilities of the regions. The results of the two LPC–PPARγ systems are compared with the Ros–PPARγ and M24–PPARγ templates in Figure 6. It is obvious that several regions (loop-1, Ω-loop, H3, β-sheet and H12) around the binding site have the large fluctuation. Thus, the key residues in the regions could affect the ligand binding. Because Ros and LPC181-2 are full agonists and would form the hydrogen bonds with Tyr473 in the H12 region, it is easy to comprehend the reduction of the H12 fluctuation for the Ros–PPARγ and LPC181-2–PPARγ complexes. In contrast, M24 and LPC181-1 are the partial agonists and do not have the strong interactions with the residues in the H12 region. The stabilization effects of M24 on β-sheet and H3 and LPC181-1 on β-sheet are remarkable. The fluctuation reduction of H12 and fluctuation increase of the Ω-loop in the LPC181-1–PPARγ systems are similar with M24–PPARγ. Previous investigation suggested that there is an allosteric network from the Ω-loop to H3 via Phe287, to H12 and consequently AF-2 surface (Waku et al., 2009). The allosteric network could cause the decrease of the H12 fluctuation in the two systems. Moreover, the ligand binding slightly decreases the β-sheet fluctuation and could influence the Ω-loop and H3 regions.

The LPC ligands analyzed here have similar backbone structure, while they are predicted to play different agonism activities. The reason is ambiguous. The possible explanation for LPC181-2 possessing the potential to be a full agonist is its double bond location and the stereoisomerism as a *trans* form. The rigidity of the double bond impedes the twisting trend of the long non-polar chain attributed from the inherent hydrophobicity. Such forced extending form of LPC181-2 thus penetrates into the Arm I region and contacts with H12 directly.

Structure alignment is a valid tool to reveal the potential mechanism of the interaction between the protein and ligand. To explore the changes of the PPARγ-LBD structure, we carefully analyze and compare the residue orientation of the PPARγ-LBD for the LPC181-1 and Ros binding. The H2′ region of the LPC181-1–PPARγ complex that connects with the Ω-loop has been driven to be away from the β-sheet (Figure 7A). Inside the cavity, LPC181-1 has bent into a 'Ω' shape and the head of such configuration oriented to the H12 without any direct interaction (Figure 4). Therefore, the H12 of the LPC181-1–PPARγ system moves outward compared with the Ros–PPARγ structure (Figure 7B). The side chains of the key residues (Arg288, Tyr327, Met329 and Met364) in the two complexes have distinct differences (Figure 7C–F). The outward movements of the residues enlarge the sphere of the ligand binding and trigger a serial of changes within the cavity. The conformation alteration of the Ω-loop in the MD simulations can be confirmed by the distribution of the

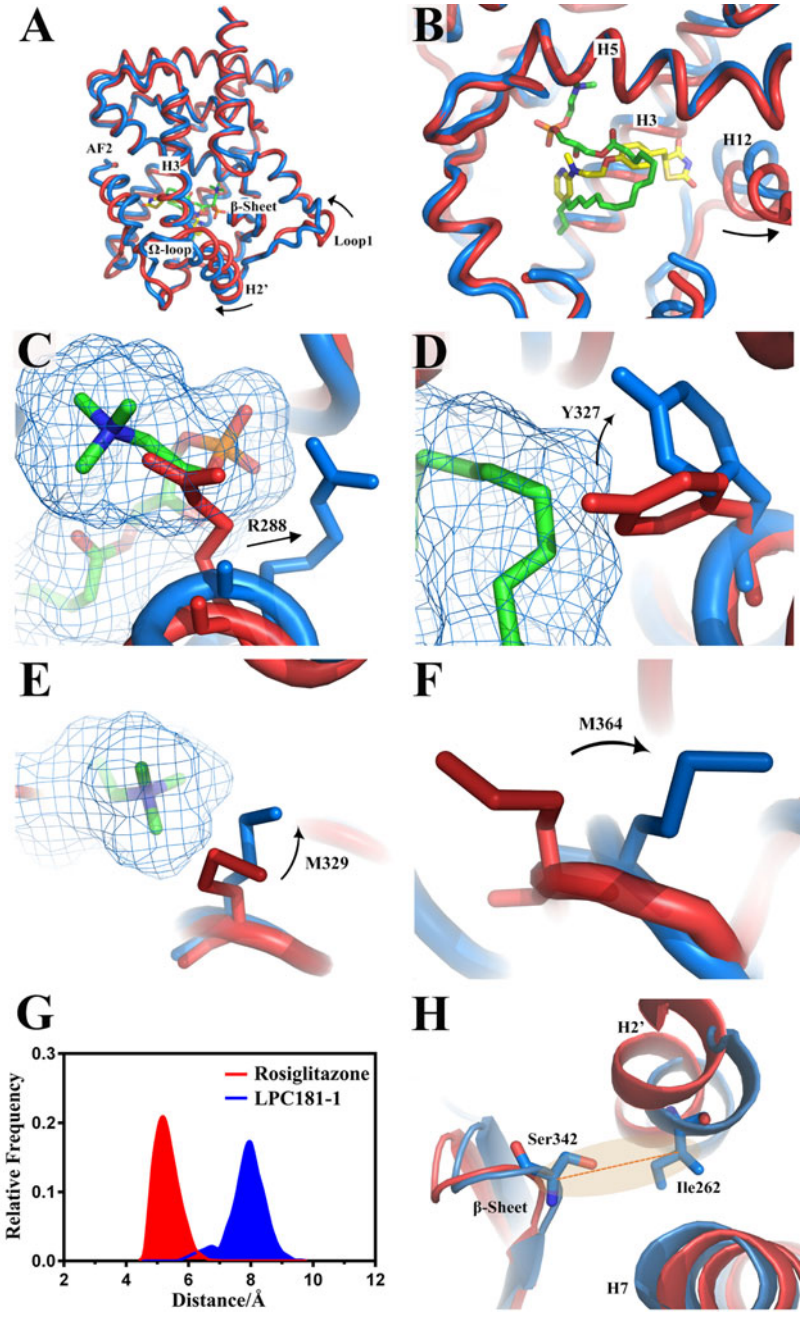

Figure 7. Structure alignment of the structures in 19.93 ns of the MD trajectories for the Ros–PPARγ and LPC181-1–PPARγ complexes. The PPARγ receptor with Ros (yellow) is shown in the red color and the PPARγ receptor with LPC181-1 (green) in the blue color. Panel G presents the distributions of the distance between the residues Ile262 (H2′) and Ser342 (β-sheet) in the 20 ns trajectories.

distance between Ile262 (H2′) and Ser342 (β-sheet). It seems that the binding of LPC181-1 drive the H2′ and Ω-loop away from the β-sheet (Figure 7G) as the distance between Ile262 and Ser342 has the larger value. Thus, the Ω-loop structure of the LPC181-1–PPARγ is obviously different from the one of Ros–PPARγ complex. Such unusual structure rearrangement makes Ω-loop special in the region mediated dynamical alteration.

Actually, there is an alternative binding site approaching the Ω-loop besides the canonical binding cavity (Hughes et al., 2014). The alterative binding of the ligand in the site would induce stabilization by the allosteric modulation via the Ω-loop mediation (Li et al., 2008). The unexpected H12 stabilization of the LPC partial agonists (LPC181-1) may mechanically emerged from the Ω-loop mediated stabilization. The long aliphatic chains of the ligand protrude into the region of the alternative binding site without the polar heads of it participating in the direct interaction with H12 (mainly Tyr473). Reference studies have addressed the distinct mechanisms of ligands increasing the magnitude of transactivation for classical pro-adipogenic genes and PPARγ-driven anti-diabetic efficacy through the expression of adiponectin enhancement (Choi et al., 2010; Choi et al., 2011). The former is directly stimulated by the region stabilization of

H12 and AF-2 which is the dominant feature of the full agonists and fundamental source of their side effects. The latter is closely related to the blockage of the phosphorylation at Ser273 (near C-terminal of the Ω-loop). The ideal PPARγ modulators of the partial agonists should preferentially block the Ser273 phosphorylation without activating AF-2 regulated gene expression to generate the anti-diabetic effects. The synthetic ligands (Ajulemic acid and Luteolin) have the ligand binding induced Ω-loop rearrangement and have been reported to acquire the remarkable insulin sensitivity with lesser unfavorable physiology effects (Ambrosio et al., 2007; Puhl et al., 2012). Among the three LPC ligands that are considered to be partial agonists in the present work, LPC181-1 has been identified to cause structure rearrangement of the Ω-loop and lesser H12 stabilization. Its role in lipid metabolism and further application as a possible parent molecule to treat the type II diabetes are thus significant and promising.

4. Conclusion

The experimental evidence had confirmed that three LPC ligands (LPC16:0, LPC18:0 and LPC18:1) can bind to the PPARγ. Here we investigate the interaction modes between the LPC ligands and PPARγ-LBD using the molecular docking and MD simulations. For each LPC–PPARγ complex, nine binding modes were first given by the molecular docking. Then, the two step MD simulations were performed to determine the final binding modes. We carried out the 20 ns MD simulations for the four LPC-PPARγ complexes and computed their binding free energies. The results of the free energies imply that present simulations are reasonable. Based on 20 ns MD simulations, we also analyzed the structures, key residues of the binding, and agonism activities for four systems.

The LDB pocket of PPARγ contains three regions named Arm I, II and III. The computational results indicate that three LPC ligands (LPC160, LPC180 and LPC181-1) bind to Arm II and III, while LPC181-2 binds to Arm I and II. The energy decomposition analysis of the key residues suggests that many residues could produce the hydrophobic interaction. They embrace the non-polar aliphatic chain of the LPC ligands. Several residues can form the stable hydrogen bonds with the LPC ligands in the MD simulation. In particular, LPC181-2 can form the hydrogen bonds with Tyr473 of H12. There is no direct interaction between other LPC ligands and Tyr473. We compared the results with the Ros–PPARγ systems as the paradigm for full agonists and with the M24–PPARγ systems for partial agonists. It can be found that LPC181-2 could be a full agonist, and LPC160, LPC180 and LPC181-1 could be the potential partial agonists. The conformational change induced by the ligand binding of the LPC partial agonists may relate to the Ω-loop mediated mechanism besides the canonical β-sheet stabilization.

Disclosure statement

The authors declare no competing financial interests or benefit.

Funding

This work was supported by National Natural Science Foundation of China under Grant 21773226.

ORCID

Yan Zhang http://orcid.org/0000-0002-7855-4375

References

Ahmadian, M., Suh, J. M., Hah, N., Liddle, C., Atkins, A. R., Downes, M., & Evans, R. M. (2013). PPARγ signaling and metabolism: The good, the bad and the future. *Nature Medicine*, *19*(5), 557. doi:10.1038/nm.3159

Al Sharif, M., Tsakovska, I., Pajeva, I., Alov, P., Fioravanzo, E., Bassan, A., … Cronin, M. T. D. (2017). The application of molecular modelling in the safety assessment of chemicals: A case study on ligand-dependent PPARγ dysregulation. *Toxicology*, *392*, 140–154. doi:10.1016/j.tox.2016.01.009

Álvarez-Almazán, S., Bello, M., Tamay-Cach, F., Martínez-Archundia, M., Alemán-González-Duhart, D., Correa-Basurto, J., & Mendieta-Wejebe, J. E. (2017). Study of new interactions of glitazone's stereoisomers and the endogenous ligand 15d-PGJ2 on six different PPAR gamma proteins. *Biochemical Pharmacology*, *142*, 168–193.

Ambrosio, A. L., Dias, S. M., Polikarpov, I., Zurier, R. B., Burstein, S. H., & Garratt, R. C. (2007). Ajulemic acid, a synthetic nonpsychoactive cannabinoid acid, bound to the ligand binding domain of the human peroxisome proliferator-activated receptor gamma. *Journal of Biological Chemistry*, *282*(25), 18625–18633. doi:10.1074/jbc.M702538200

Atanasov, A. G., Wang, J. N., Gu, S. P., Bu, J., Kramer, M. P., Baumgartner, L., … Heiss, E. H. (2013). Honokiol: A non-adipogenic PPARγ agonist from nature. *Biochimica et Biophysica Acta*, *1830*(10), 4813–4819. doi:10.1016/j.bbagen.2013.06.021

Bayly, C. I., Cieplak, P., Cornell, W., & Kollman, P. A. (1993). A well-behaved electrostatic potential based method using charge restraints for deriving atomic charges: the RESP model. *The Journal of Physical Chemistry*, *97*(40), 10269–10280. doi:10.1021/j100142a004

Becke, A. D. (1992). Density-functional thermochemistry. 1. The effect of the exchange-only gradient correction. *Journal of Chemical Physics*, *96*(3), 2155–2160. doi:10.1063/1.462066

Becke, A. D. (1993). Density-functional thermochemistry. 3. The role of exact exchange. *Journal of Chemical Physics*, *98*(7), 5648–5652. doi:10.1063/1.464913

Biasini, M., Bienert, S., Waterhouse, A., Arnold, K., Studer, G., Schmidt, T., … Schwede, T. (2014). SWISS-MODEL: Modelling protein tertiary and quaternary structure using evolutionary information. *Nucleic Acids Research*, *42*(W1), W252–W258. doi:10.1093/nar/gku340

Bruning, J. B., Chalmers, M. J., Prasad, S., Busby, S. A., Kamenecka, T. M., He, Y., … Griffin, P. R. (2007). Partial agonists activate PPARγ using a helix 12 independent mechanism. *Structure*, *15*(10), 1258–1271. doi:10.1016/j.str.2007.07.014

Chawla, A., Repa, J. J., Evans, R. M., & Mangelsdorf, D. J. (2001). Nuclear receptors and lipid physiology: Opening the X-files. *Science (New York, N.Y.)*, *294*(5548), 1866. doi:10.1126/science.294.5548.1866

Choi, J. H., Banks, A. S., Estall, J. L., Kajimura, S., Boström, P., Laznik, D., … Spiegelman, B. M. (2010). Anti-diabetic drugs inhibit obesity-linked phosphorylation of PPARgamma by Cdk5. *Nature*, *466*(7305), 451–456. doi:10.1038/nature09291

Choi, J. H., Banks, A. S., Kamenecka, T. M., Busby, S. A., Chalmers, M. J., Kumar, N., … Griffin, P. R. (2011). Antidiabetic actions of a non-agonist PPARgamma ligand blocking Cdk5-mediated phosphorylation. *Nature*, *477*(7365), 477–481.

D. A., Case, D. S., Cerutti, T. E., Cheatham, I. T. A., Darden, R. E., Duke, T. J., Giese, … Kollman, P. A. (2017). *AMBER 16*. San Francisco: University of California.

Day, C. (1999). Thiazolidinediones: A new class of antidiabetic drugs. *Diabetic Medicine* , *16*(3), 179–192.

Ditchfield, R., Hehre, W. J., & Pople, J. A. (1971). Self-consistent molecular-orbital methods. 9. Extended Gaussian-type basis for molecular-orbital studies of organic molecules. *Journal of Chemical Physics*, *54*(2), 724. doi:10.1063/1.1674902

Dolinsky, T. J., Czodrowski, P., Li, H., Nielsen, J. E., Jensen, J. H., Klebe, G., & Baker, N. A. (2007). PDB2PQR: Expanding and upgrading automated preparation of biomolecular structures for molecular simulations. *Nucleic Acids Research*, *35*(Web Server), W522–W525. doi:10.1093/nar/gkm276

Essmann, U., Perera, L., Berkowitz, M. L., Darden, T., Lee, H., & Pedersen, L. G. (1995). A smooth particle mesh Ewald method. *The Journal of Chemical Physics*, *103*(19), 8577–8593. doi:10.1063/1.470117

Genheden, S., Akke, M., & Ryde, U. (2014). Conformational entropies and order parameters: Convergence, reproducibility, and transferability. *Journal of Chemical Theory and Computation*, *10*(1), 432–438. doi:10.1021/ct400747s

Hughes, T. S., Giri, P. K., de Vera, I. M. S., Marciano, D. P., Kuruvilla, D. S., Shin, Y., … Kojetin, D. J. (2014). An alternate binding site for PPARγ ligands. *Nature Communications*, *5*, 3571–3571.

Jia, W.-Q., Jing, Z., Liu, X., Feng, X.-Y., Liu, Y.-Y., Wang, S.-Q., … Cheng, X.-C. (2018). Virtual identification of novel PPARα/γ dual agonists by scaffold hopping of saroglitazar. *Journal of Biomolecular Structure and Dynamics*, *36*(13), 3496–3512. doi:10.1080/07391102.2017.1392363

Jorgensen, W. L., Chandrasekhar, J., Madura, J. D., Impey, R. W., & Klein, M. L. (1983). Comparison of simple potential functions for simulating liquid water. *The Journal of Chemical Physics*, *79*(2), 926–935. doi:10.1063/1.445869

Kollman, P. A., Massova, I., Reyes, C., Kuhn, B., Huo, S., Chong, L., … Cheatham, T. E. (2000). Calculating structures and free energies of complex molecules: Combining molecular mechanics and continuum models. *Accounts of Chemical Research*, *33*(12), 889–897. doi:10.1021/ar000033j

Kroker, A. J., & Bruning, J. B. (2015). Review of the structural and dynamic mechanisms of PPARγ partial agonism. *PPAR Research*, *2015*, 816856doi:10.1155/2015/816856

Kuhn, B., & Kollman, P. A. (2000). Binding of a diverse set of ligands to avidin and streptavidin: An accurate quantitative prediction of their relative affinities by a combination of molecular mechanics and continuum solvent models. *Journal of Medicinal Chemistry*, *43*(20), 3786–3791. doi:10.1021/jm000241h

Lauber, K., Bohn, E., Kröber, S. M., Xiao, Y-J., Blumenthal, S. G., Lindemann, R. K., … Wesselborg, S. (2003). Apoptotic cells induce migration of phagocytes via caspase-3-mediated release of a lipid attraction signal. *Cell*, *113*(6), 717–730. doi:10.1016/S0092-8674(03)00422-7

Lee, C., Yang, W., & Parr, R. G. (1988). Development of the Colle-Salvetti correlation-energy formula into a functional of the electron density. *Physical Review B*, *37*(2), 785–789. doi:10.1103/PhysRevB.37.785

Lee, W., Ham, J., Kwon, H. C., Kim, Y. K., & Kim, S.-N. (2013). Anti-diabetic effect of amorphastilbol through PPARα/γ dual activation in db/db mice. *Biochemical and Biophysical Research Communications*, *432*(1), 73–79. doi:10.1016/j.bbrc.2013.01.083

Lehrke, M., & Lazar, M. A. (2005). The many faces of PPARgamma. *Cell*, *123*(6), 993–999. doi:10.1016/j.cell.2005.11.026

Li, X., Fang, P., Li, Y., Kuo, Y.-M., Andrews, A. J., Nanayakkara, G., … Yang, X. (2016). Mitochondrial reactive oxygen species mediate lysophosphatidylcholine-induced endothelial cell activation. *Arteriosclerosis, Thrombosis, and Vascular Biology*, *36*(6), 1090–1100. doi:10.1161/ATVBAHA.115.306964

Liu, X., Jing, Z., Jia, W.-Q., Wang, S.-Q., Ma, Y., Xu, W.-R., … Cheng, X.-C. (2018). Identification of novel PPARα/γ dual agonists by virtual screening, ADMET prediction and molecular dynamics simulations. *Journal of Biomolecular Structure and Dynamics*, *36*(11), 2988–3002.

Li, X., Shao, Y., Sha, X., Fang, P., Kuo, Y.-M., Andrews, A. J., … Yang, X. (2018). IL-35 (Interleukin-35) suppresses endothelial cell activation by inhibiting mitochondrial reactive oxygen species-mediated site-specific acetylation of H3K14 (Histone 3 Lysine 14). *Arteriosclerosis, Thrombosis, and Vascular Biology*, *38*(3), 599–609. doi:10.1161/ATVBAHA.117.310626

Li, Y., Wang, Z., Furukawa, N., Escaron, P., Weiszmann, J., Lee, G., … Chen, J.-L. (2008). T2384, a novel antidiabetic agent with unique peroxisome proliferator-activated receptor γ binding properties. *Journal of Biological Chemistry*, *283*(14), 9168–9176. doi:10.1074/jbc.M800104200

Li, Y., Zhang, J., Schopfer, F. J., Martynowski, D., Garcia-Barrio, M. T., Kovach, A., … Xu, H. E. (2008). Molecular recognition of nitrated fatty acids by PPARγ. *Nature Structural & Molecular Biology*, *15*, 865. doi:10.1038/nsmb.1447

Lindorff-Larsen, K., Piana, S., Palmo, K., Maragakis, P., Klepeis, J. L., Dror, R. O., & Shaw, D. E. (2010). Improved side-chain torsion potentials for the Amber ff99SB protein force field. *Proteins: Structure, Function, and Bioinformatics*, *78*(8), 1950–1958. doi:10.1002/prot.22711

Frisch, M. J., Trucks, G. W., Schlegel, H. B., Scuseria, G. E., Robb, M. A., Cheeseman, J. R., Fox, … J. (2010). *Gaussian 09, revision D.1*. Wallingford, CT: Gaussian, Inc.

Miller, B. R., McGee, T. D., Swails, J. M., Homeyer, N., Gohlke, H., & Roitberg, A. E. (2012). MMPBSA.py: An efficient program for end-state free energy calculations. *Journal of Chemical Theory and Computation*, *8*(9), 3314–3321. doi:10.1021/ct300418h

Muñoz-Gutiérrez, C., Sepúlveda, C., Caballero, J., Palomo, I., & Fuentes, E. (2017). Study of the interactions between edaglitazone and ciglitazone with PPARγ and their antiplatelet profile. *Life Sciences*, *186*, 59–65. doi:10.1016/j.lfs.2017.07.031

Mueller, M., & Jungbauer, A. (2008). Red clover extract: A putative source for simultaneous treatment of menopausal disorders and the metabolic syndrome. *Menopause*, *15*(6), 1120–1131. doi:10.1097/gme.0b013e31817062ce

Muralikumar, S., Vetrivel, U., Narayanasamy, A., & N. Das, U. (2017). Probing the intermolecular interactions of PPARγ-LBD with polyunsaturated fatty acids and their anti-inflammatory metabolites to infer most potential binding moieties. *Lipids in Health and Disease*, *16*(1), 17.

Nissen, S. E., & Wolski, K. (2007). Effect of rosiglitazone on the risk of myocardial infarction and death from cardiovascular causes. *The New England Journal of Medicine*, *356*(24), 2457–2471. doi:10.1056/NEJMoa072761

Nolte, R. T., Wisely, G. B., Westin, S., Cobb, J. E., Lambert, M. H., Kurokawa, R., … Milburn, M. V. (1998). Ligand binding and co-activator assembly of the peroxisome proliferator-activated receptor-γ. *Nature*, *395*(6698), 137. doi:10.1038/25931

Pearson, S. L., Cawthorne, M. A., Clapham, J. C., Dunmore, S. J., Holmes, S. D., Moore, G. B. T., … Tadayyon, M. (1996). The thiazolidinedione insulin sensitiser, BRL 49653, increases the expression of PPAR-gamma and aP2 in adipose tissue of high-fat-fed rats. *Biochemical and Biophysical Research Communications*, *229*(3), 752–757. doi:10.1006/bbrc.1996.1876

Puhl, A. C., Bernardes, A., Silveira, R. L., Yuan, J., Campos, J. L. O., Saidemberg, D. M., … Polikarpov, I. (2012). Mode of peroxisome proliferator-activated receptor γ activation by luteolin. *Molecular Pharmacology*, *81*(6), 788. doi:10.1124/mol.111.076216

Qin, Q., Wang, B., Wang, J., Chang, M., Xia, T., Shi, X., & Xu, G. (2019). A comprehensive strategy for studying protein-metabolite interactions by metabolomics and native mass spectrometry. *Talanta*, *194*, 63–72. doi:10.1016/j.talanta.2018.10.010

Ryckaert, J.-P., Ciccotti, G., & Berendsen, H. J. C. (1977). Numerical integration of the Cartesian equations of motion of a system with constraints: Molecular dynamics of n-alkanes. *Journal of Computational Physics*, *23*(3), 327–341. doi:10.1016/0021-9991(77)90098-5

Schupp, M., & Lazar, M. A. (2010). Endogenous ligands for nuclear receptors: Digging deeper. *Journal of Biological Chemistry*, *285*(52), 40409–40415. doi:10.1074/jbc.R110.182451

Sharifi, T., & Ghayeb, Y. (2018). A computational study to identify the key residues of peroxisome proliferator-activated receptor gamma in the interactions with its antagonists. *Journal of Biomolecular Structure and Dynamics*, *36*(7), 1822–1833. doi:10.1080/07391102.2017.1335618

Singh, S., & Mohanty, A. (2018). In silico identification of potential drug compound against Peroxisome proliferator-activated receptor-gamma by virtual screening and toxicity studies for the treatment of Diabetic

Nephropathy. *Journal of Biomolecular Structure and Dynamics*, *36*(7), 1776–1787. doi:10.1080/07391102.2017.1334596

Sun, H., Duan, L., Chen, F., Liu, H., Wang, Z., Pan, P., … Hou, T. (2018). Assessing the performance of MM/PBSA and MM/GBSA methods. 7. Entropy effects on the performance of end-point binding free energy calculation approaches. *Physical Chemistry Chemical Physics*, *20*(21), 14450–14460.

Takada, I., & Makishima, M. (2015). PPARγ ligands and their therapeutic applications: A patent review (2008 – 2014). *Expert Opinion on Therapeutic Patents*, *25*(2), 175–191. doi:10.1517/13543776.2014.985206

Trott, O., & Olson, A. J. (2010). AutoDock Vina: Improving the speed and accuracy of docking with a new scoring function, efficient optimization, and multithreading. *Journal of Computational Chemistry*, *31*, 455–461. doi:10.1002/jcc.21334

Tsakovska, I., Al Sharif, M., Alov, P., Diukendjieva, A., Fioravanzo, E., Cronin, M. T. D., & Pajeva, I. (2014). Molecular modelling study of the PPARγ receptor in relation to the mode of action/adverse outcome pathway framework for liver steatosis. *International Journal of Molecular Sciences*, *15*(5), 7651–7666. doi:10.3390/ijms15057651

Waku, T., Shiraki, T., Oyama, T., Fujimoto, Y., Maebara, K., Kamiya, N., … Morikawa, K. (2009). Structural insight into PPARgamma activation through covalent modification with endogenous fatty acids. *Journal of Molecular Biology*, *385*(1), 188–199. doi:10.1016/j.jmb.2008.10.039

Wang, J., Wolf, R. M., Caldwell, J. W., Kollman, P. A., & Case, D. A. (2004). Development and testing of a general amber force field. *Journal of Computational Chemistry*, *25*(9), 1157–1174. doi:10.1002/jcc.20035

Wang, L., Waltenberger, B., Pferschy-Wenzig, E.-M., Blunder, M., Liu, X., Malainer, C., … Atanasov, A. G. (2014). Natural product agonists of peroxisome proliferator-activated receptor gamma (PPARγ): A review. *Biochemical Pharmacology*, *92*(1), 73–89. doi:10.1016/j.bcp.2014.07.018

Weidner, C., de Groot, J. C., Prasad, A., Freiwald, A., Quedenau, C., Kliem, M., … Sauer, S. (2012). Amorfrutins are potent antidiabetic dietary natural products. *Proceedings of the National Academy of Sciences of United States of America*, *109*(19), 7257–7262. doi:10.1073/pnas.1116971109

Weidner, C., Wowro, S. J., Freiwald, A., Kawamoto, K., Witzke, A., Kliem, M., … Sauer, S. (2013). Amorfrutin B is an efficient natural peroxisome proliferator-activated receptor gamma (PPARγ) agonist with potent glucose-lowering properties. *Diabetologia*, *56*(8), 1802–1812. doi:10.1007/s00125-013-2920-2

Zoete, V., Grosdidier, A., & Michielin, O. (2007). Peroxisome proliferator-activated receptor structures: Ligand specificity, molecular switch and interactions with regulators. *Biochimica et Biophysica Acta (BBA) - Molecular and Cell Biology of Lipids*, *1771*(8), 915–925. doi:10.1016/j.bbalip.2007.01.007